

Document downloaded from:

<http://hdl.handle.net/10251/49160>

This paper must be cited as:

Gomis Hilario, O.; Vilaplana Cerda, Rl.; Manjón, F.; Santamaría Pérez, D.; Errandonea, D.; Pérez González, E.; López Solano, J.... (2013). Crystal structure of HgGa₂Se₄ under compression. *Materials Research Bulletin*. 48:2128-2133.
doi:10.1016/j.materresbull.2013.02.037.



The final publication is available at

<http://www.sciencedirect.com/science/article/pii/S0025540813001220>

Copyright Elsevier

Crystal structure of HgGa₂Se₄ under compression

Oscar Gomis,^{a,*} Rosario Vilaplana,^a Francisco Javier Manjón,^b David Santamaría-Pérez,^{c,d} Daniel Errandonea,^d Eduardo Pérez-González,^e Javier López-Solano,^e Plácida Rodríguez-Hernández,^e Alfonso Muñoz,^e Ion Mihail Tiginyanu,^f and Veaceslav Vladimir Ursaki^f

^aCentro de Tecnologías Físicas: Acústica, Materiales y Astrofísica, MALTA Consolider Team, Universitat Politècnica de València, 46022 València, Spain

^bInstituto de Diseño para la Fabricación y Producción Automatizada, MALTA Consolider Team, Universitat Politècnica de València, 46022 València, Spain

^cDepartamento de Química Física I, Universidad Complutense de Madrid, MALTA Consolider Team, Avenida Complutense s/n, 28040 Madrid, Spain

^dDepartamento de Física Aplicada-ICMUV, MALTA Consolider Team, Universidad de Valencia, Edificio de Investigación, C/Dr. Moliner 50, Burjassot, 46100 Valencia, Spain

^eDepartamento de Física Fundamental II, Instituto de Materiales y Nanotecnología, MALTA Consolider Team, Universidad de La Laguna, 38205 Tenerife, Spain

^fInstitute of Applied Physics, Academy of Sciences of Moldova, 2028 Chisinau, Moldova

* Corresponding author. Tel.: +34 96 652 8426; fax: +34 96 652 8485.

E-mail address: osgohi@fis.upv.es (Oscar Gomis)

Dr. Oscar Gomis

Departamento de Física Aplicada

Escuela Politécnica Superior de Alcoy

Universitat Politècnica de València

Placeta Ferrandiz Carbonell 2

03802 Alcoy (Alicante)

Spain

Abstract

We report on high-pressure x-ray diffraction measurements up to 17.2 GPa in mercury digallium selenide (HgGa_2Se_4). The equation of state and the axial compressibilities for the low-pressure tetragonal phase have been determined and compared to related compounds. HgGa_2Se_4 exhibits a phase transition on upstroke towards a disordered rock-salt structure beyond 17 GPa, while on downstroke it undergoes a phase transition below 2.1 GPa to a phase that could be assigned to a metastable zinc-blende structure with a total cation-vacancy disorder. Thermal annealing at low- and high-pressure shows that kinetics plays an important role on pressure-driven transitions.

Keywords:

- A. Chalcogénides
- C. High-pressure
- C. X-ray diffraction
- D. Crystal structure
- D. Phase transitions

PACS numbers: 61.05.cp, 61.50.Ks, 62.50.-p, 64.70.kg

56 **1. Introduction**

57

58 Mercury digallium selenide (HgGa_2Se_4) is one of the less studied adamantine-
59 type $A^{\text{II}}B_2^{\text{III}}X_4^{\text{VI}}$ ordered-vacancy compounds (OVCs). It crystallizes in the tetragonal
60 defect-chalcopyrite (DC) structure with space group (SG) I-4, $Z=2$ [see **Fig. 1(a)**].
61 Adamantine OVCs are tetrahedrally-coordinated semiconductors which have an
62 unoccupied cationic site [**1, 2**]. The presence of vacancies results in a complex physics
63 and explains why OVCs have been scarcely studied. A common feature of them is that
64 they have several non-equivalent tetrahedrally-coordinated cations resulting in a
65 distortion of the crystal lattice from the cubic symmetry. This fact, their anisotropy, and
66 their band-gap energies make them suitable for many technological applications [**3, 4**].

67 High-pressure (HP) studies on $A^{\text{II}}B_2^{\text{III}}X_4^{\text{VI}}$ compounds are receiving increasing
68 attention in the last years [**3-20**]. In particular, ternary selenide compounds have been
69 recently studied [**3, 4, 6 - 10, 12 - 20**]. However, to our knowledge, only one work has
70 been devoted to HgGa_2Se_4 [**3**], being focused on optical properties. In order to improve
71 the knowledge of the HP behaviour of $AGa_2\text{Se}_4$ compounds, we report here synchrotron
72 XRD measurements in HgGa_2Se_4 . In particular, we show evidence of the presence of
73 two new phases. They can be probably assigned to a disordered rock-salt (DR) structure
74 (SG: Fm-3m, $Z=1$) [see **Fig. 1(b)**] and a disorder zinc-blende (DZ) structure (SG: F-
75 43m, $Z=1$) [see **Fig. 1(c)**].

76

77 **2. Experimental section**

78 Single crystals of DC- HgGa_2Se_4 have been grown from its constituents HgSe
79 and Ga_2Se_3 by chemical vapor transport method using iodine as a transport agent [**21**].
80 Chemical and structural analyses have shown the stoichiometric composition of the

81 crystals and no spurious phases have been observed. Ambient pressure x-ray diffraction
82 and Raman spectroscopy confirmed that our sample has a DC-type structure.

83 We have carried out a HP angle-dispersive powder x-ray diffraction (XRD)
84 experiment at room temperature. This experiment was performed up to 17.2 GPa at
85 beamline ID27 of ESRF using a monochromatic beam ($\lambda = 0.3738 \text{ \AA}$) with a beam
86 diameter of 5 μm full-width at half maximum. In this experiment samples were loaded
87 in a modified Merrill-Basset diamond anvil cell (DAC) allowing access to an angular
88 range of $2\theta = 25^\circ$. HgGa_2Se_4 powder was placed in the 150 μm -diameter hole of a
89 stainless-steel gasket pre-indented to a thickness of 50 μm . XRD images were collected
90 using a MARCCD detector located at 238 mm away from the sample and then
91 integrated and corrected for distortions using FIT2D [22]. The typical acquisition time
92 was 10 s. In this case samples were loaded in the DAC with MgO which was used both
93 as the pressure-transmitting medium (PTM) and as pressure marker using its equation of
94 state (EOS): $B_0 = 154.7 \text{ GPa}$, and $B_0' = 4.69$ [23]. We select the use of this pressure
95 medium because the non-hydrostatic conditions thus generated favor the occurrence of
96 phase transitions [24, 25]. The indexing and refinement of the powder patterns were
97 performed using the UNITCELL [26], POWDERCELL [27] and GSAS program
98 packages [28, 29].

99

100 **3. Results and discussion**

101

102 **Figure 2** shows selected XRD patterns of DC- HgGa_2Se_4 from ambient pressure
103 till 17.2 GPa obtained in our experiment on increasing and decreasing pressure.
104 Asterisks mark the peaks corresponding to MgO. **Table 1** summarizes the lattice
105 parameters and atomic positions of DC- HgGa_2Se_4 , obtained at 1 bar from a Rietveld

106 refinement of our XRD pattern. The refined parameters were: the scale factor, lattice
107 parameters, profile coefficients, fractional coordinates of the Se anion, and the overall
108 displacement factor. The background was subtracted previously. Our results agree with
109 those of **Refs. 30** and **31** which are also shown in **Table 1** for comparison.

110 In **Fig. 2** diffractograms from 1 bar to 17.2 GPa on upstroke correspond to the
111 low-pressure tetragonal DC phase and show that diffraction peaks move to higher
112 angles as pressure increases, thus indicating that the interplanar distances decrease. It is
113 also observed that peak widths of the DC-HgGa₂Se₄ phase increase gradually above 7
114 GPa which implies that hydrostatic conditions are deteriorating with increasing
115 pressure. On the other hand, in general, HgGa₂Se₄ peaks move faster than those of MgO
116 as can be seen from the (111) MgO Bragg reflection located at 8.93° at 7.1 GPa. This
117 reflection is overtaken at 10.1 GPa by the (211) DC-HgGa₂Se₄ Bragg reflection located
118 at 8.71° at 1 bar. This fact is a consequence of the different compressibility of MgO and
119 HgGa₂Se₄. At 17.2 GPa all peaks broaden considerably and two new broad peaks
120 appear (see + marks). We have interpreted this result as a signature of the onset of a
121 non-reversible phase transition. In order to release strain in the sample at 17.2 GPa we
122 annealed the sample (393 K during 1 hour) using an external heater [32]. After thermal
123 treatment, pressure decreased slightly (16.2 GPa) and the new XRD pattern showed
124 some remnant peaks from the initial DC phase and a major proportion of a new phase
125 that can be assigned to the DR structure phase previously proposed for related
126 compounds [10, 16-19]. According to the relation of intensities of Bragg peaks of both
127 phases [33], we can estimate that an 85% of the sample was transformed to the HP
128 phase. Unfortunately, the DAC we used prevented us from going to higher pressures. A
129 Rietveld refinement of the diffractogram measured at 16.2 GPa at the upstroke which
130 shows the coexistence of the DR and DC phases along with MgO is included in **Fig. 2**.

131 The multiphase Rietveld gives the same result for the amount of sample transformed to
132 the HP phase. **Table 2** summarizes the crystallographic parameters of DR-HgGa₂Se₄ at
133 16.2 GPa. The quality of the structural refinement is similar for the pattern collected at
134 16.2 GPa after annealing than for the pattern collected at 1 bar (see **Fig. 2** and residuals
135 in **Tables 1** and **2**).

136 On decompression we took several XRD patterns showing the coexistence of
137 DR and DC phases till 5.7 GPa, with the DR phase being in all cases the dominant one.
138 Below 5.7 GPa the peaks of the HP phase disappear and broad XRD peaks appear as
139 shown in the spectrum of **Fig. 2** at 2.1 GPa (solid line) on downstroke. As we will
140 discuss below, apparently the changes observed in the XRD pattern can be assigned to a
141 transition to a phase different than the low- and high-pressure phases previously
142 described. The XRD patterns of this new phase can be attributed to a DZ structure.
143 Again, in order to release strain, we annealed the recovered sample at 2.1 GPa (393 K
144 during 30 minutes). After thermal treatment, pressure decreased to 1.5 GPa and the new
145 XRD pattern showed a well-defined tetragonal structure, which proved to be similar to
146 the structure of the low-pressure phase, but with broader peaks that could evidence
147 some degree of disorder in the sample. A plausible hypothesis that can explain this
148 phenomenon is that the cation and vacancy disorder caused during the DC-to-DR
149 transition cannot be reordered upon decompression resulting in the appearance of a
150 metastable DZ phase on decompression. The additional energy provided by the thermal
151 annealing helps to reduce disorder and relax stresses favoring the recovery of the
152 thermodynamically stable low-pressure phase. A DZ structure has been already found in
153 CdGa₂Se₄ [10], CdAl₂Se₄ [17], CdAl₂S₄ [19], and HgAl₂Se₄ [19] on decreasing pressure
154 from the DR structure.

155 As mentioned above, a detailed study of the XRD pattern obtained on
156 downstroke at 2.1 GPa before annealing evidence the presence of a possible metastable
157 phase with DZ structure. In **Figure 2** it is shown the comparison of the diffraction
158 pattern measured upon decompression at 2.1 GPa (solid line) and the calculated pattern
159 (dash-dotted line) for a DZ phase. A lattice parameter of 5.45(1) Å provides the best
160 matching to the new peaks assigned to the DZ structure. To facilitate comparison of
161 both diffractograms, the background was subtracted in the measured one and the
162 simulated diffractogram was modeled with profile parameters obtained by comparison
163 to the measured one using the Powdercell software. The resemblance of both
164 experimental and calculated diffractograms is quite good. The broad aspect of the
165 allowed zinc-blende diffraction Bragg reflections is likely to be a consequence of the
166 complete disorder of cations and vacancies at the only cation site (4a Wyckoff position)
167 in the metastable zinc-blende structure (see **Table 2**).

168 We would like to mention here that because of the broad bands of the diffraction
169 pattern measured at 2.1 GPa and the fact that some of the Bragg peaks attributed to the
170 DZ phase have quite a low intensity a structural refinement cannot be performed. Note
171 also, that because the high symmetry of both the DR and DZ structures a maximum of 6
172 to 8 Bragg peaks of them can be detected working in a diamond-anvil cell even using
173 short wavelength like in this work. This fact also precludes the performance of a proper
174 structural refinement even for simple structures like DR and DZ in which neither atom
175 possesses any internal degree of freedom. In previous works, both phases have been
176 identified in related compounds with less than six reflections, but not proper structural
177 refinements were carried out [10, 17, 19] All these facts indicate that in the future it will
178 be necessary to carry out single-crystal XRD experiments [34] in order to properly
179 determine the crystal structure of the new HP phases observed in OVCs. Another

180 interesting issue to explore in the future is the role of kinetics. The fact that thermal
181 annealing is requested for completion of the transitions triggered by compression or
182 decompression shows that kinetical barriers could be relevant in the studied transitions.
183 On the other hand, our observation of a tetragonal phase at 1.5 GPa after heating a
184 decompressed sample with DZ structure at 2.1 GPa is compatible with previous studies
185 that show a recrystallization of the DC structure in $Zn_{1-x}Mn_xGa_2Se_4$ after a moderate
186 heating of samples with the defect stannite structure, which already has some degree of
187 disorder, above 300°C in vacuum and decreasing temperature in a controlled way [35,
188 36].

189 **Figure 3** shows the pressure dependence of the lattice parameters for DC-
190 $HgGa_2Se_4$ from our experiment. The axial compressibilities for a and c axes at zero
191 pressure, defined as $\kappa_x = \frac{-1}{x} \frac{\partial x}{\partial P}$ and obtained by fitting of a Murnaghan EOS to
192 experimental data [37], are $\kappa_a = 9(2) \cdot 10^{-3} \text{ GPa}^{-1}$ and $\kappa_c = 5(1) \cdot 10^{-3} \text{ GPa}^{-1}$. It can be
193 observed that there is an anisotropy in the axial compression being the a axis more
194 compressible than the c one. This result agrees with previous results for related
195 compounds [10, 16, 18, 19, 38].

196 **Figure 4** shows the volume of the DC phase vs. pressure plot obtained from our
197 experiment (circles). Experimental data for the DR phase on downstroke and the DZ
198 phase at 2.1 GPa are shown as diamonds and squares, respectively. We have fitted our
199 volume vs. pressure data for the DC phase with a third order Birch-Murnaghan EOS
200 [39]. The fitting of the data of Fig. 4 (dashed line) with a volume at zero pressure fixed
201 at a value of $V_0 = 352.70(16) \text{ \AA}^3$ (the measured value at ambient pressure) and the bulk
202 modulus pressure derivative at zero pressure fixed at a value of $B_0' = 4$ gives a bulk
203 modulus of $B_0 = 52(2) \text{ GPa}$. The EOS parameters are summarized in **Table 3** together
204 with parameters obtained from a different experiment carried out with a laboratory

205 diffractometer using methanol-ethanol as pressure transmitting medium to reduce
206 deviatoric stresses and in a reduced pressure range (13.2 GPa) to avoid the influence of
207 precursor effects [40] of the pressure-driven transition on the structure of the low-
208 pressure phase [38]. If we compare the obtained value for B_0 when B_0' is fixed to 4 for
209 both experiments, it can be seen that the B_0 for the experiment when MgO is used as
210 PTM is about 16% greater than that B_0 obtained when methanol-ethanol is used as
211 PTM. This result confirms the overestimation of B_0 under non-hydrostatic conditions
212 noted in previous works [24, 25, 41, 42, 43]. Finally, we note that the obtained value for
213 B_0 in DC-HgGa₂Se₄ from our experiment with MgO as PTM is similar to that obtained
214 for DC-CdGa₂Se₄ ($B_0 = 41.5(2)$ GPa) [10], DC-MnGa₂Se₄ ($B_0 = 44(2)$ GPa) [16], DC-
215 CdAl₂Se₄ ($B_0 = 52.1$ GPa) [17], and DS-ZnGa₂Se₄ ($B_0 = 47(2)$ GPa) [18].

216 As regards the DR phase, it can be observed from **Fig. 4** that it is less
217 compressible than the DC phase. We have estimated a relative volume change per
218 formula unit of -2.2% at 16.2 GPa, thus indicating that the DC to DR phase transition is
219 a first-order phase transition of reconstructive nature. A fit of our experimental volume
220 vs. pressure data for the DR phase with a Birch-Murnaghan EOS with B_0' fixed to 4
221 gives a bulk modulus of $B_0 = 103(6)$ GPa and a volume at zero pressure $V_0 = 159.9(8)$
222 \AA^3 . The greater value for the B_0 of the DR phase in comparison to that of the DC phase
223 confirms the lower compressibility of the HP phase. The same result is found for other
224 OVCs like MnGa₂Se₄, CdAl₂S₄ and ZnGa₂Se₄ [16, 18, 19]. If we compare the
225 normalized volumes of the DC, DR, and DZ phases at 2.1 GPa it is found that the
226 volume of the DZ phase [$324(2) \text{\AA}^3$] is between those of the DC [$338(3) \text{\AA}^3$] and DR
227 [$314(2) \text{\AA}^3$] phases. In the comparison, the volume for the DR phase at 2.1 GPa has
228 been extrapolated by using the EOS, and in the cases of the DR and DZ volume was
229 normalized multiplying by two. The volume of the three phases decreases in the

230 sequence $DC > DZ > DR$ which suggest that the compressibility of the DZ structure
231 should be in between those of the other two phases since the packing efficiency of DZ is
232 in between those of DC and DR.

233 Now we will analyze the evolution of the c/a ratio with pressure in DC-
234 HgGa_2Se_4 since the tetragonal distortion, $\delta = 2 - c/a$, could give important information
235 about the behavior of the sample on compression. Inset of **Fig. 4** shows the pressure
236 dependence of the c/a ratio vs. pressure. It can be observed that c/a increases with
237 increasing pressure from 1.89 at ambient pressure to 1.94 at 17.3 GPa. A similar
238 experimental pressure dependence of the c/a ratio has been found in CdGa_2Se_4 [10],
239 MnGa_2Se_4 [16], CdGa_2S_4 [18], HgAl_2Se_4 [19], and in HgGa_2Se_4 [38] under better
240 hydrostatic conditions than here. It is noteworthy that AGa_2X_4 compounds ($A = \text{Mn, Zn,}$
241 $\text{Cd, Hg; } X = \text{S, Se}$) with tetragonal DC structure at ambient pressure have c/a values
242 close to 1.90 [10, 16, 38, 44], while those with tetragonal defect stannite structure like
243 ZnGa_2Se_4 or ZnGa_2S_4 , which have already some cation disorder, have c/a ratios close to
244 1.98 at ambient pressure [18, 45]. Furthermore, a c/a ratio very close to 2, or
245 equivalently a very small tetragonal distortion of the tetragonal phase, has been
246 considered up to now as a measure of complete cation-vacancy disorder [31, 44].
247 Therefore, our results show that DC- HgGa_2Se_4 , like other DC compounds [4, 10, 16],
248 tends to a more symmetrical structure on compression prior to undergoing the phase
249 transition to the DR structure at 17.2 GPa.

250 To conclude we would like to comment on the different coordination found on
251 the DC, DR, and DZ structures shown in **Fig 1**. The low pressure DC phase has four-
252 fold coordination where cations are tetrahedrally-coordinated while anions are
253 surrounded by three cations and a vacancy. The high pressure DR phase has six-fold
254 coordination where cations and anions are octahedrally-coordinated. In this way, the

255 phase transition implies an increase of the symmetry of the crystal and is accompanied
256 by a change of coordination of the cations from tetrahedral to octahedral. On the other
257 hand, the metastable DZ phase has again four-fold coordination as the original DC
258 phase.

259

260 **4. Summary**

261 We have performed XRD measurements in defect chalcopyrite HgGa_2Se_4 under
262 compression. The experiments show that the pressure dependence of the volume and
263 lattice parameters of DC- HgGa_2Se_4 behaves in a similar way to other adamantine
264 OVCs. The axial compressibilities and the equation of state of HgGa_2Se_4 have been
265 obtained for the tetragonal DC structure under non-hydrostatic conditions. It is observed
266 that the tetragonal structures of OVCs tend to become more symmetric under
267 compression irrespective of the conditions of hydrostaticity. A non-reversible phase
268 transition to the disordered rock-salt phase on increasing pressure has been found. On
269 decreasing pressure the sample was found to undergo a phase transition to a metastable
270 structure that might be attributed to a disordered zinc-blende structure. Apparently
271 kinetics plays an important role on the occurrence of the reported phase transitions. This
272 is evidenced by the fact that thermal annealing favors the occurrence of phase
273 transitions.

274 **Acknowledgements**

275 This study was supported by the Spanish government MEC under Grants No:
276 MAT2010-21270-C04-01/03/04 and CTQ2009-14596-C02-01, by the Comunidad de
277 Madrid and European Social Fund (S2009/PPQ-1551 4161893), by MALTA Consolider
278 Ingenio 2010 project (CSD2007-00045), and by the Vicerrectorado de Investigación y

279 Desarrollo of the Universidad Politécnica de Valencia (UPV2011-0914 PAID-05-11
280 and UPV2011-0966 PAID-06-11). E.P-G., J.L-S., A.M., and P.R-H. acknowledge
281 computing time provided by Red Española de Supercomputación (RES) and MALTA-
282 Cluster.

283

284 **References**

- 285 [1] A. MacKinnon, in Tables of Numerical Data and Functional Relationships in
286 Science and Technology, edited by O. Madelung, M. Schulz, and H. Weiss, Landolt-
287 Börnstein New Series, Group III, Vol. 17, pt. h (Springer-Verlag, Berlin, 1985) p. 124.
- 288 [2] J.E. Bernard and A. Zunger, Phys. Rev. B **37** (1988) 6835.
- 289 [3] F.J. Manjón, O. Gomis, P. Rodríguez-Hernández, E. Pérez-González, A. Muñoz, D.
290 Errandonea, J. Ruiz-Fuertes, A. Segura, M. Fuentes-Cabrera, I. Tiginyanu, and V.V.
291 Ursaki, Phys. Rev. B **81** (2010) 195201.
- 292 [4] O. Gomis, R. Vilaplana, F. J. Manjón, E. Pérez-González, J. López-Solano, P.
293 Rodríguez-Hernández, A. Muñoz, D. Errandonea, J. Ruiz-Fuertes, A. Segura, D.
294 Santamaría-Pérez, I. M. Tiginyanu, and V.V. Ursaki, Journal of Appl. Phys. **111** (2012)
295 013518.
- 296 [5] I. I. Burlakov, Y. Raptis, V. V. Ursaki, E. Anastassakis, and I. M. Tiginyanu, Solid
297 State Commun. **101** (1997) 377.
- 298 [6] J. González, R. Rico, E. Calderón, M. Quintero, and M. Morocoima, phys. stat. sol.
299 (b) **211** (1999) 45.
- 300 [7] V.V. Ursaki, I.I. Burlakov, I.M. Tiginyanu, Y.S. Raptis, E. Anastassakis, and A.
301 Anedda, Phys. Rev. B **59** (1999) 257.
- 302 [8] M. Fuentes-Cabrera and O.F. Sankey, J. Phys.: Condens. Matter **13**, (2001) 1669.
- 303 [9] M. Fuentes-Cabrera, J. Phys.: Condens. Matter **13** (2001) 10117.
- 304 [10] A. Grzechnik, V.V. Ursaki, K. Syassen, I. Loa, I.M. Tiginyanu, and M. Handfland,
305 J. Solid State Chem. **160**, (2001) 205.

- 306 [11] T. Mitani, S. Onari, K. Allakhverdiev, F. Gashimzade, and T. Kerimova, *phys. stat.*
307 *sol. (b)* **223** (2001) 287.
- 308 [12] A. Tatsi, D. Lampakis, E. Liarokapis, S.A. López, L. Martínez, and W. Giriat, *High*
309 *Press. Res.* **22** (2002) 89.
- 310 [13] I. M. Tiginyanu, V.V. Ursaki, F.J. Manjón, and V.E. Tezlevan, *J. Phys. Chem.*
311 *Solids* **64**, (2003) 1603.
- 312 [14] T. Mitani, T. Naitou, K. Matsuishi, S. Onari, K. Allakhverdiev, F. Gashimzade, and
313 T. Kerimova, *phys. stat. sol. (b)* **235** (2003) 321.
- 314 [15] K. Allakhverdiev, F. Gashimzade, T. Kerimova, T. Mitani, T. Naitou, K.
315 Matsuishi, and S. Onari, *J. Phys. Chem. Solids* **64**, (2003) 1597.
- 316 [16] J. Marquina, Ch. Power, P. Grima, M. Morocoima, M. Quintero, B. couzinet, J.C.
317 Chervin, P. Munsch, and J. González, *J. Appl. Phys.* **100** (2006) 093513.
- 318 [17] S. Meenakshi, V. Vijyakumar, B.K. Godwal, A. Eifler, I. Orgzall, S. Tkachev, and
319 H.D. Hochheimer, *J. Phys. Chem. Solids* **67** (2006) 1660.
- 320 [18] D. Errandonea, R.S. Kumar, F.J. Manjón, V.V. Ursaki, and I.M. Tiginyanu, *J.*
321 *Appl. Phys.* **104** (2008) 063524.
- 322 [19] S. Meenakshi, V. Vijyakumar, A. Eifler, and H.D. Hochheimer, *J. Phys. Chem.*
323 *Solids* **71** (2010) 832.
- 324 [20] P. Singh, M. Sharma, U.P. Verma, and P. Jensen, *Z. Kristallogr.* **225** (2010) 508.
- 325 [21] I.M. Tiginyanu, N. A. Modovyan, and O. D. Stoika, *Fiz. Tverd. Tela* **34** (1992) 967
326 (1992); *idem*, *Sov. Phys. Solid State* **43** (1992) 527.

- 327 [22] A. P. Hammersley, S. O. Svensson, M. Hanfland, A. N. Fitch, and D. Häusermann,
328 High Pressure Research, **14** (1996) 235.
- 329 [23] P. I. Dorogokupets, and A. Dewaele, High Pressure Research **27** (2007) 431.
- 330 [24] J. Ruiz-Fuertes, D. Errandonea, R. Lacomba-Perales, A. Segura, J. González, F.
331 Rodríguez, F. J. Manjón, S. Ray, P. Rodríguez-Hernández, A. Muñoz, Zh. Zhu, and C.
332 Y. Tu, Phys. Rev. B, **81** (2010) 224115.
- 333 [25] O. Gomis, J. A. Sans, R. Lacomba-Perales, D. Errandonea, Y. Meng, J. C. Chervin,
334 and A. Polian, Phys. Rev. B, **86** (2012) 054121.
- 335 [26] T. J. B. Holland, and S. A. T. Redfern, Mineralogical Magazine, **61** (1997) 65.
- 336 [27] W. Kraus and G. Nolze, J. Appl. Crystallogr. **29** (1996) 301.
- 337 [28] A. C. Larson and R. B. von Dreele, LANL Report 86-748, 2004 (unpublished).
- 338 [29] B. H. Toby, J. Appl. Cryst. **34** (2001) 210.
- 339 [30] H. Hahn, G. Frank, W. Klingler, A.D. Stoerger, and G. Stoerger, Zeitschrift fuer
340 Anorganische und Allgemeine Chemie **279** (1955) 241.
- 341 [31] L. Gastaldi, M.G. Simeone, and S. Viticoli, Solid State Commun. **55** (1985) 605.
- 342 [32] D. Errandonea, D. Martínez-García, A. Segura, A. Chevy, G. Tobias, E. Canadell,
343 and P. Ordejon, Phys. Rev. B **73** (2006) 235202.
- 344 [33] D. Errandonea, R. Boehler, S. Japel, M. Mezouar, and L. R. Benedetti, Phys. Rev.
345 B **73** (2006) 092106.

- 346 [34] J. Ruiz-Fuertes, A. Friedrich, J. Pellicer-Porres, D. Errandonea, A. Segura, W.
347 Morgenroth, E. Haussühl, C.-Y. Tu, and A. Polian, *Chemistry of Materials* **23** (2011)
348 4220.
- 349 [35] P. Alonso-Gutiérrez, M.L. Sanjuán, and M.C. Morón, *phys. Stat. sol. (c)* **6** (2009)
350 1182. P. Alonso-Gutiérrez, Ph. D. thesis, University of Zaragoza (2009), unpublished.
- 351 [36] D. Caldera, M. Morocoima, M. Quintero, C. Rincón, R. Casanova, and P. Grima,
352 *Solid State Commun.* **151** (2011) 212.
- 353 [37] M. D. Frogley, J. L. Sly, and D. J. Dunstan, *Phys. Rev. B* **58** (1998) 12579.
- 354 [38] O. Gomis, R. Vilaplana, F.J. Manjón, D. Santamaría-Pérez, D. Errandonea, E.
355 Pérez-González, J. López-Solano, P. Rodríguez-Hernández, A. Muñoz, I. M. Tiginyanu,
356 and V. V. Ursaki, submitted to *Journal of Applied Physics*.
- 357 [39] F. Birch, *J. Geophys. Res.* **83** (1978) 1257.
- 358 [40] E. Bandiello, D. Errandonea, D. Martinez-Garcia, D. Santamaria-Perez, and F. J.
359 Manjon, *PRB* **85** (2012) 024108.
- 360 [41] H.Z Liu, Y. Ding, M. Somayazulu, J. Qian, J. Shu, D. Häusermann, and H.K. Mao,
361 *Phys. Rev. B* **71** (2005) 212103.
- 362 [42] H.Z. Liu, J.Z. Hu, J.F. Shu, D. Häusermann, and H.K. Mao, *Appl. Phys. Lett.* **85**
363 (2004) 1973.
- 364 [43] D. Santamaría-Pérez, L. Gracia, G. Garbarino, A. Beltrán, R. Chulia-Jordan, O.
365 Gomis, D. Errandonea, Ch. Ferrer-Roca, D. Martínez-García, and A. Segura, *Phys. Rev.*
366 *B* **84** (2011) 054102.
- 367 [44] L. Garbato, F. Ledda, and A. Rucci, *Prog. Cryst. Growth Charact.* **15** (1987) 1.

368 [45] C. K. Lowe-Ma and T.A. Vanderah, *Acta Cryst. C* **47** (1991) 919.

369

370 **Table 1.** Experimental crystallographic parameters of tetragonal (I-4, Z=2) HgGa₂Se₄ at
 371 room conditions. The residuals for the Rietveld refinement are R_p= 11% and R_{wp}
 372 =16.4%.

373

	X-ray diffraction ^a	X-ray diffraction ^b	X-ray diffraction ^c
<i>a</i> (Å)	5.711(1)	5.715	5.693(1)
<i>c</i> (Å)	10.814(1)	10.78	10.826(4)
Hg site: 2 <i>a</i>	x=0 y=0 z=0	x=0 y=0 z=0	x=0 y=0 z=0
Ga(1) site: 2 <i>b</i>	x = 0 y = 0 z = 0.5	x = 0 y = 0 z = 0.5	x = 0 y = 0 z = 0.5
Ga(2) site: 2 <i>c</i>	x = 0 y = 0.5 z = 0.25	x = 0 y = 0.5 z = 0.25	x = 0 y = 0.5 z = 0.25
Vacancy site: 2 <i>d</i>	x = 0 y = 0.5 z = 0.75	x = 0 y = 0.5 z = 0.75	x = 0 y = 0.5 z = 0.75
Se site: 8 <i>g</i>	x = 0.270(2) y = 0.245(5) z = 0.1315(6)	x = 0.25 y = 0.25 z = 0.125	x = 0.273(1) y = 0.2582(8) z = 0.1382(6)

374

375 ^a Our XRD experiment. ^b Reference 30. ^c Reference 31.

376

377

378

379 **Table 2.** Experimental crystallographic parameters of DR (Fm-3m, Z=1) HgGa₂Se₄ at
 380 16.2 GPa. The lattice parameter is $a = 5.2048(5)$ Å. The residuals for the Rietveld
 381 refinement are $R_p = 9.8\%$ and $R_{wp} = 13.4\%$. We also include the atomic positions used
 382 to simulate DZ-HgGa₂Se₄ (F-43m, Z=1) at 2.1 GPa with $a = 5.45(1)$ Å.

383

	DR-HgGa ₂ Se ₄		DZ-HgGa ₂ Se ₄	
	Wyckoff position	Site occupancy factor (S.O.F.)	Wyckoff position	Site occupancy factor (S.O.F.)
Hg	4a (0,0,0)	0.25	4a (0,0,0)	0.25
Ga	4a (0,0,0)	0.5	4a (0,0,0)	0.5
Vacancy	4a (0,0,0)	0.25	4a (0,0,0)	0.25
Se	4b (1/2,1/2,1/2)	1	4c (1/4,1/4,1/4)	1

384

385

386

387 **Table 3:** Experimental (exp.) volume (V_0), bulk modulus (B_0), and its pressure
 388 derivative (B_0') for DC-HgGa₂Se₄ at ambient pressure. Values were obtained by fitting
 389 data to a third-order Birch-Murnaghan EOS with B_0' fixed to 4 and V_0 fixed to the
 390 value measured at 1 bar. Data from **Ref. 38** are also included for comparison.

391

	V_0 (\AA^3)	B_0 (GPa)	B_0'	References
exp.	352.70	52(2)	4 (fixed)	This work
exp.	352.9(6)	39(2)	5.2(4)	38
	351.4(5)	44.9(7)	4 (fixed)	

392

393

394 **Figure captions**

395

396 **Figure 1. (Color online)** (a) Structure of the defect chalcopyrite (DC) HgGa_2Se_4 , (b)
397 defect rock salt (DR) HgGa_2Se_4 , and (c) defect zinc blende (DZ) HgGa_2Se_4 . Big light
398 atoms are Hg, medium dark atoms are Ga, and small dark atoms are Se. To distinguish
399 between nonequivalent atoms in the DC structure, the Wyckoff sites are given in
400 parenthesis.

401 **Figure 2.** XRD patterns of HgGa_2Se_4 on upstroke up to 17.2 GPa and downstroke to 1.5
402 GPa. The diffractogram measured at 1 bar at the upstroke is shown as solid circles. The
403 calculated pattern at 1 bar obtained from a Rietveld refinement along with the residuals
404 are shown as solid lines. A Rietveld refinement of the diffractogram measured at 16.2
405 GPa at the upstroke showing the coexistence of the DR and DC phases along with MgO
406 is included. The residuals are $R_p = 9.8\%$ and $R_{wp} = 13.4\%$. In the pattern collected at 2.1
407 GPa on downstroke, we show the comparison of the measured pattern (solid line) and
408 the calculated diffractogram using Powdercell software for the defect zincblende (DZ)
409 phase (dash-dotted line). Vertical marks indicate the Bragg reflections for the DC phase
410 at 1 bar at the upstroke, for the DR and DC phases and MgO at 16.2 GPa at the
411 upstroke, and for the DZ phase at 2.1 GPa at the downstroke. Plus (+) symbols refer to
412 reflections attributed to the disordered rocksalt phase and MgO reflections are marked
413 with * symbols.

414 **Figure 3.** Lattice parameters of the DC phase of HgGa_2Se_4 as a function of pressure.
415 Solid and empty circles refer to data from our XRD experiment on increasing and
416 decreasing pressure, respectively. Solid lines are a guide to the eye.

417 **Figure 4.** Volume of the DC (circles) and DR (diamonds) phases as a function of
418 pressure. The volume of the DZ phase at 2.1 GPa is included as square symbols. Full
419 symbols are used for upstroke and empty symbols for downstroke. Note that for
420 comparison of the three structures we have plotted twice the volume of the DR and DZ
421 phases since the unit cell of DC phase has $Z = 2$ while that of the DR and DZ phases has
422 $Z=1$. Dashed and dash-dotted lines are the result of the EOS fit for the DC and DR
423 phases of our experiment. Inset: Evolution of the c/a ratio of the DC phase as a function
424 of pressure for our experiments (circles). Dashed line is a linear fit to experimental data.

Figure 1.

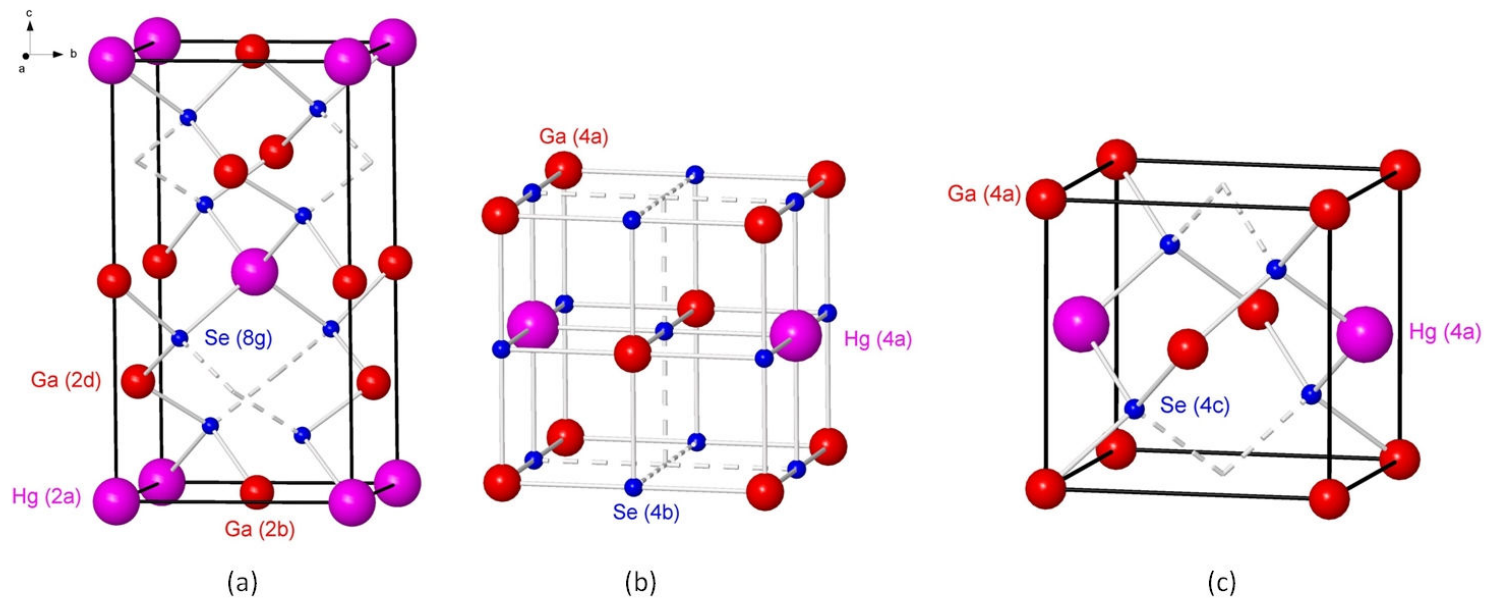


Figure 2

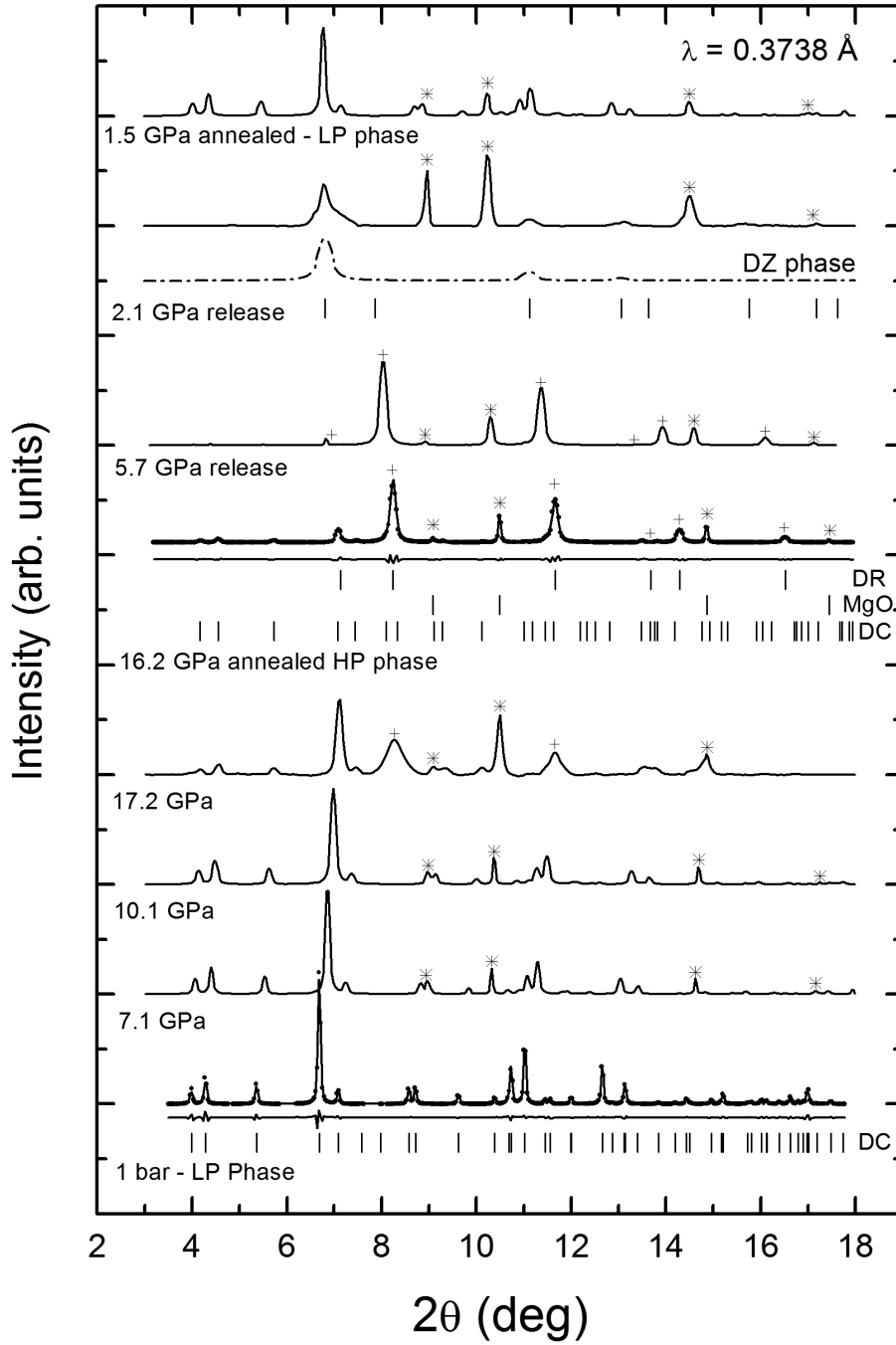


Figure 3

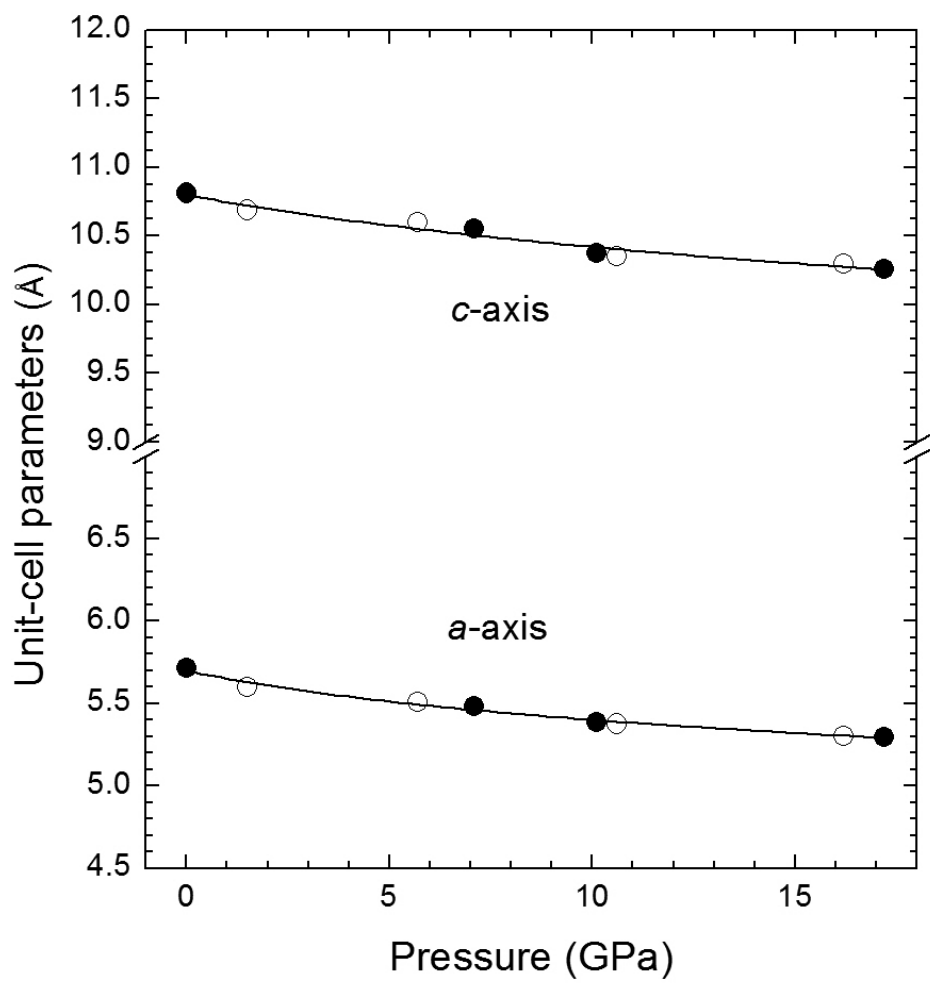


Figure 4

